HHS Public Access

Author manuscript

J Vis Exp. Author manuscript; available in PMC 2022 December 16.

Biological Preparation and Mechanical Technique for Determining Viscoelastic Properties of Zonular Fibers

Juan Rodriguez[1,2], **Matthew Reilly**[3], **Robert P. Mecham**[4], **Steven Bassnett**[2,4]

[1]Department of Basic Sciences, University of Health Sciences and Pharmacy

[2]Department of Ophthalmology & Visual Sciences, Washington University School of Medicine

[3]Department of Biomedical Engineering, The Ohio State University

[4]Department of Cell Biology & Physiology, Washington University School of Medicine

Abstract

Elasticity is essential to the function of tissues such as blood vessels, muscles, and lungs. This property is derived mostly from the extracellular matrix (ECM), the protein meshwork that binds cells and tissues together. How the elastic properties of an ECM network relate to its composition, and whether the relaxation properties of the ECM play a physiological role, are questions that have yet to be fully addressed. Part of the challenge lies in the complex architecture of most ECM systems and the difficulty in isolating ECM components without compromising their structure. One exception is the zonule, an ECM system found in the eye of vertebrates. The zonule comprises fibers hundreds to thousands of micrometers in length that span the cell-free space between the lens and the eyewall. In this report, we describe a mechanical technique that takes advantage of the highly organized structure of the zonule to quantify its viscoelastic properties and to determine the contribution of individual protein components. The method involves dissection of a fixed eye to expose the lens and the zonule and employs a pull-up technique that stretches the zonular fibers equally while their tension is monitored. The technique is relatively inexpensive yet sensitive enough to detect alterations in viscoelastic properties of zonular fibers in mice lacking specific zonular proteins or with aging. Although the method presented here is designed primarily for studying ocular development and disease, it could also serve as an experimental model for exploring broader questions regarding the viscoelastic properties of elastic ECM's and the role of external factors such as ionic concentration, temperature, and interactions with signaling molecules

Introduction

The eye of a vertebrate contains a living optical lens that helps focus images on the retina[1] . The lens is suspended on the optical axis by a system of delicate, radially-oriented fibers, as illustrated in Figure 1A. At one end, the fibers attach to the lens equator and, at the

Corresponding Author: Juan Rodriguez Juan.Rodriguez@uhsp.edu.

A complete version of this article that includes the video component is available at http://dx.doi.org/10.3791/63171.

Disclosures

The authors have nothing to disclose.

other, to the surface of the ciliary body. Their lengths span distances ranging from 150 μm in mice to 1 mm in humans. Collectively, these fibers are known as the zonule of Zinn[2], the ciliary zonule, or simply the zonule. Ocular trauma, disease, and certain genetic disorders can affect the integrity of the zonular fibers[3] , resulting in their eventual failure and accompanying loss of vision. In mice, the fibers have a core comprised mostly of the protein fibrillin-2, surrounded by a mantle rich in fibrillin-1[4]. Although zonular fibers are unique to the eye, they bear many similarities to elastin-based ECM fibers found elsewhere in the body. The latter are covered by a fibrillin-1 mantle[5] and have similar dimensions to zonular fibers[6]. Other proteins, such as latent- transforming growth factor β-binding proteins (LTBPs) and microfibril-associated glycoprotein-1 (MAGP-1), are found in association with both types of fibers[7, 8, 9, 10, 11]. The elastic modulus of zonular fibers is in the range of 0.18-1.50 MPa[12, 13, 14, 15, 16], comparable to that of elastin-based fibers (0.3-1.2 MPa)[17]. These architectural and mechanical similarities lead us to believe that any insight into the roles of zonule-associated proteins may help elucidate their roles in other ECM elastic fibers.

The main purpose of developing the method described here is to gain insights into the role of specific zonular proteins in the progression of inherited eye disease. The general approach is to compare the viscoelastic properties of zonular fibers in wild-type mice with those of mice carrying targeted mutations in genes encoding zonular proteins. While several methods have been used previously to measure the elasto-mechanical properties of zonular fibers, all were designed for the eyes of much larger animals[12, 13, 14, 15, 16]. As such models are not genetically tractable; we sought to develop an experimental method that was better suited to the small and delicate eyes of mice.

The method we developed for assessing the viscoelasticity of mouse zonular fibers is a technique we refer to as the pull- up assay[4, 18], which is summarized visually in Figure 1. A detailed description of the pull-up method and the analysis of the results is provided below. We begin by describing the construction of the apparatus, including the three-dimensional (3D)-printed parts used in the project. Next, we detail the protocol used for obtaining and preparing the eyes for the experiment. Lastly, we provide step-by-step instructions on how to obtain data for the determination of the viscoelastic properties of zonular fibers. In the Representative Results section, we share previously unpublished data obtained with our method on the viscoelastic properties of zonular fibers from mice lacking MAGP-1[19] as well as a control set obtained from age-matched wild-type animals. Finally, we conclude with general remarks on the advantages and limitations of the method, and suggestions for potential experiments that may elucidate how environmental and biochemical factors affect the viscoelastic properties of ECM fibers.

Protocol

All animal experiments were approved by the Washington University Animal Studies Committee and adhered to the ARVO Statement for the Use of Animals in Ophthalmic and Vision Research.

1. Fabrication of specialized parts and construction of apparatus

1. Fabrication of specialized parts

    1. Probe fabrication. Hold a glass capillary at an angle as shown in the left panel of Figure 2A. Place a flame from a cigarette lighter about 2 cm from one end and keep it there until the end bends by 90°, as shown in the right panel of Figure 2A.

    2. Sample platform fabrication. Using 3D drawing software, design a platform measuring 30 x 30 x 5 mm and containing hemispherical indentations of 2.0, 2.5, and 3.0 mm in diameter, as shown in Figure 2B.

    3. Probe holder fabrication. Using the 3D drawing software, design a mount that holds the capillary probe and attach it to a micromanipulator (see Figure 2C).

        NOTE: A sample 3D file for platform fabrication and probe holder fabrication in STL format is available on request from the corresponding author.

    4. Negative lens assembly. Place a negative cylindrical lens (−75 mm in focal length and approximately 50 mm in height and length) as shown in Figure 1C and Figure 1D to correct the distortion caused by the addition of fluid to the Petri dish (addition of fluid distorts the view of the dissected eye when imaged from the side).

    5. Glue the negative lens to one of the 2-slotted bases (see Figure 2D for positioning of the lens on the base).

    6. Assemble the remaining parts as shown in Figure 2D.

    7. Adjust the height of the post so that the lens barely hovers over the scale and tighten the screw in the post-holder.

2. Construction of apparatus

    1. Install on a computer the logging program supplied with the scale, the microscope camera software, and the motorized micrometer controller application.

    2. Connect the motorized micrometer to the servo motor controller and the latter to the computer. Start the motor controller application and edit the motor settings.

        NOTE: The motor settings, which are listed below, were chosen following preliminary experiments that revealed that stresses relaxed on a time scale of 10-20 s. Based on this determination, we selected a speed and acceleration that allowed the motor to complete a 50 μm displacement in a time smaller than the relaxation time, but not too short to avoid jolting the sample. Here we chose a displacement time of about 5-10 s.

3. Set the maximum velocity to 0.01 mm/s and the acceleration to 0.005 mm/s2.

4. Install the camera in the inspection microscope and test the camera imaging software.

5. Place the scale on the bench space devoted to the apparatus.

6. Glue a 3D-printed platform (from step 1.1.2) to a Petri dish and add a 2-3 mm glass bead to one of the wells. Place the Petri dish on the scale so that the bead is located near the center of the pan.

7. Replace the manual micrometer from the micromanipulator with the motorized one.

8. Screw the two 4-40 screws into the probe holder. Attach the probe holder to the manipulator as shown in Figure 1C.

9. Prepare a probe as illustrated in Figure 2A, place it inside the probe holder with the bent portion facing down, and tighten the screws.

10. Position the micromanipulator on the table such that the tip of the probe is over the bead on the platform. Affix the micromanipulator to the table to prevent accidental movement during the experiment.

11. Position the side microscope on the table so that the bead is at the center of its field of view and in focus.

2. Sample preparation and data acquisition

1. Eye fixation and dissection

    1. Maintain wild-type mice and *Magp1*-null animals on an identical C57/BL6J background. Euthanize 1- month-old or 1-year-old mice by CO_2 inhalation.

    2. Remove the eyes with fine forceps and fix the enucleated globes at 4 °C overnight in 4% paraformaldehyde/phosphate-buffered saline (PBS, pH 7.4). Maintain a positive pressure of 15-20 mmHg in the eye during the fixation process, as described[6]. NOTE: Experiments are conducted on male mice, to control for possible sex-related differences in the size of the ocular globe. The positive pressure ensures that the globe remains inflated, preserving the gap between the lens and the wall of the eye spanned by the zonular fibers.

    3. Wash the eyes for 10 min in PBS. Using ophthalmic surgical scissors and working under a stereomicroscope, make a full-thickness incision in the wall of the eye near the optic nerve head.

    4. Extend the cut forward to the equator, and then around the equatorial circumference of the eye.Take care to spare the delicate ciliary processes and associated zonular fibers.

5. Remove the back of the globe, exposing the posterior surface of the lens.

6. Use the forceps to remove a dissected eye from the buffer solution and place it on a dry task wipe with the cornea facing down. Gently drag the cornea over the surface of the wipe to dry it.

7. Add 3 μL of instant glue to the platform wells that will accommodate the eye in the Petri dish.

8. Place the dish on the stage plate of the stereomicroscope so that the well with the glue is in view.

9. Transfer the eye from the wipe to the edge of the well that contains glue. Then, carefully drag the eye into the well and quickly adjust its orientation so that the back of the lens is uppermost.

10. Dry the exposed side of the lens by gently blotting it with the corner of a dry wipe.

11. Apply a dab of instant glue to the bottom of a 50 mm Petri dish and cement the platform to it.

2. Measurement of zonular viscoelastic response

1. Turn on the scale, start the scale logging program and the camera software. Ensure that the logging program can acquire data for 30 min, as some trials can last that long.

2. Switch on the servo motor controller and start the controller application on the computer. Make sure the controller is set to move in 50 μm increments using motion parameters similar to those outlined in the NOTE in step 1.2.2.

3. Create a 90° bend in a capillary rod as described in step 1.1.1.

4. Slip the bent capillary into the capillary probe holder and tighten the securing screws.

   NOTE: To minimize sample dehydration, we recommend that steps 1-4 be completed prior to, or during, eye dissection.

5. Add a small (~1 mm) bead of UV-curing glue to the tip of the capillary.

6. Using the manual adjustments on the manipulator, move the tip of the capillary probe so that it is directly over the center of the lens. Check whether the bottom portion of the UV glue appears centered over the top of the lens when viewed from the front (by visual inspection) and the side (through the microscope camera).

7. While looking through the camera, lower the probe tip until the UV glue makes contact with the lens and covers one-third to one-half of its upper surface.

8. Use a low-intensity (~ 1 mW), directional, near- visible UV (380-400 nm) light source to cure the glue. NOTE: These specifications suffice to cure the glue in a few seconds while minimizing the potential for inducing protein crosslinking. The UV light sources supplied with commercial UV glue pens meet these specifications.

9. Add PBS solution to the dish until the eye is covered by fluid to a depth of at least 2 mm.

10. Place the cylindrical lens in front of the inspection microscope and as close as possible to the Petri dish without touching it.

11. Simultaneously start the logging program and a timer program. Take a picture of the eye/probe using the camera.

12. After 60 s, initiate another 50 μm displacement, and thereafter every 60 s until the experiment is complete, i.e., until all the fibers have been broken. Note that the signal will not return to baseline levels due to buffer evaporation during the experiment. Correct the ensuing drift in the readings during the data analysis, as exemplified in step 2.2.14.

13. Upon completion of a run, save the scale logging data and export it into a format compatible with the spreadsheet, e.g., a .csv format. Save the lens pictures that were collected during the run.

14. Import data into a spreadsheet. Use the first and the last scale reading to interpolate the drift in the background reading over time due to evaporation (see Figure 3). Subtract the interpolated reading from the reading at each time point.

    NOTE: If using a spreadsheet, the interpolation can be performed automatically by entering the formula = B2 − B2 + (B2 − @INDIRECT("B•&COUNTA(B:B)))/(COUNTA(B:B)-2) * A2 in the cell to the right of the first scale reading, then moving the cursor to the right-lower corner of the cell and dragging it down to the last data value. The formula assumes that the data is organized in a column with the first data point appearing in cell B2. If desired, the data processed in step 2.2.14 may be analyzed with the quasi-elastic viscoelastic model developed by one of the co-authors, Dr. Matthew Riley[4].

Representative Results

The pull-up technique described here provides a straightforward approach for determining viscoelastic properties of zonular fibers in mice. In brief, the mouse eye is first preserved by injection of a fixative at physiological intraocular pressure. This approach maintains the natural inflation of the eye and keeps the fibers properly pre- tensioned (fixation was deemed acceptable after preliminary experiments demonstrated it did not alter the elasticity or strength of the fibers significantly). The back of the mouse eye is then removed by dissection to expose the lens and the zonular fibers that suspend it. The front of the eye

is affixed to a platform and placed inside a Petri dish that rests on a digital scale. Next, a glass capillary attached to a micromanipulator is cemented to the posterior surface of the lens. The lens is then raised in 50 μm increments while the force on the scale is recorded. A reduction in the apparent weight of the preparation provides information about the forces that stretch the fibers. Each displacement is followed by an equilibration period lasting about 1 min to observe any relaxation of the stress induced by the displacement. Finally, the results are analyzed using a quasi-linear viscoelastic model designed specifically for the geometry of the mouse zonular fibers and the direction of the pull in for the assay[4].

Typical viscoelastic data obtained with our method are shown in Figure 3. The curve appears inverted (negative) since the lift force on the lens reduces the weight of the dish/platform/eye assembly on the scale by an equivalent amount. The response includes instantaneous force spikes during each of the 50 μm vertical displacements of the lens, followed by a relaxation phase with a lifetime on the order of 10 s. A similar stress relaxation has been observed for bovine zonular fibers[12]. The magnitude of the instantaneous and relaxed forces increases with each step up to about 1000 s (~800 μm total displacement) and then begins to drop as fibers start to fail. Zonule failure is complete by the 1,500 s time point (~1.25 mm total displacement). Note that due to the evaporation of buffer in the course of the experiment, the curve does not return to the initial reading after the lens is freed from the eye.

Figure 4 contrasts the responses obtained for a *Magp-1* knockout mouse (red curve) and an age-matched wild-type animal (blue curve). These curves have been corrected for evaporation, inverted, and the raw measurements of mass (see Figure 3) are now expressed as force (with units of mN). The initial viscoelastic response of the *Magp-1*-depleted zonule (time 0-600 s) closely resembles that of the wild-type, suggesting that the viscoelastic properties of the zonule were not significantly altered by the absence of *Magp-1*. However, the fibers appear to rupture at a much lower tension compared to their wild-type counterparts.

To illustrate the reliability of the method, we gathered data from multiple animals on the maximum instantaneous force applied to the eyes before their fibers ruptured. The results are shown in Figure 5. The data for 1-month-old mice exhibit very small values for the standard error of the mean (SEM) despite the relatively low number of samples used (n = 5 or 6), suggesting high reproducibility. The results indicate that the strength of the fibers differs significantly between the two genotypes (p-value = 2.4 x 10^{-6}). Results not shown in the figures also suggest that there is a subtle but statistically significant increase in breaking force strength with age for wild-type animals (p-value = 0.024).

The pull-up method also can generate quantitative estimates of the viscoelastic parameters that account for the observed variations in temporal responses. Table 1 summarizes best- fit parameters to our MAGP-1 data, obtained with a quasi-linear viscoelastic model described previously[4]. The results show that both MAGP-1 deletion and aging can have highly significant impacts on some of the mechanical properties of zonular fibers.

Discussion

The zonule is an unusual ECM system where fibers are arranged symmetrically and can be manipulated identically by displacing the eye lens along the optical axis. The space can also be readily accessed without cellular disruption, allowing the fibers to be studied in an environment close to their native state. The pull-up technique takes advantage of this ECM presentation to manipulate the delicate fibers from mice, a genetically tractable system, and accurately quantify their mechanical properties. This has allowed us to examine the contribution of key ECM proteins (fibrillin-1[18], LTBP-2[4], and MAGP-1 reported here) to the biomechanical properties of the zonular fibers. Our analysis of fibrillin-1-deficient mice revealed that zonular fibers lacking fibrillin-1 weaken with age and eventually rupture, leading to the displacement of the lens within the eye (in humans, a condition known as ectopia lentis). Significantly, lens dislocation is also a common occurrence in patients with Marfan syndrome, a disease caused by mutations in the *FBN1* gene[20]. Thus, the pull-up assay offers an opportunity to model aspects of human connective tissue disease in mice. In mice lacking LTPB-2 (a protein thought to be involved in the genesis of microfibrils), we were able to demonstrate that zonular fibers were produced in the absence of that protein, but ruptured at significantly lower stresses and eventually disintegrated with age[4]. These results suggest that LTBP-2 contributes to the longevity of the fibers rather than their synthesis. In the current study, we determined that MAGP-1-deficient fibers had similar viscoelastic properties to wild-type fibers but ruptured at lower stresses, with no sign of further age- related degradation. This would be consistent with a model in which fibers lacking MAGP-1 are intrinsically weaker as soon as they develop.

We note that the ultimate tensile strengths listed in Table 1 are estimated under the assumption that the fibers break somewhere mid-span. However, we cannot rule out the possibility that fiber failure is due to detachment from anchorage points on the lens surface or the ciliary body. If this were the case, the fracture tensile strength of the fiber could be higher than the values listed in Table 1. Microscopic analysis will be required to differentiate between these possibilities. Such analysis is far from trivial since the fibers involved are very thin (~0.5-0.6 μm in width) and nearly index-matched to water, making them essentially invisible. In the absence of this additional information, we can only state that the ultimate tensile strengths listed in Table 1 represent their lower limits. It would also be interesting, in principle, to check whether the force measurements differ depending on which direction the lens is pulled. In practice, however, pulling the lens from the anterior side would require removing the iris without damaging the zonular fibers lying immediately beneath. Such precise dissection is beyond what we can currently achieve with the mouse eye.

The relative simplicity of the method and the high reproducibility of its results are desirable qualities for comparative studies of ECM mechanical properties. Additionally, as demonstrated here, it is also possible to use the pull-up assay to obtain absolute values of viscoelastic parameters by assuming a viscoelastic model and fitting the time curves to it. For instance, using a standard quasi-linear viscoelastic (QLV) model, we were able to extract values for instantaneous (G_0) and equilibrium (G_∞) stiffnesses, the relaxation time constant (τ), and the ultimate tensile strength (σ_f) of zonular fibers from wild-type mice, as well as those lacking LTBP-2[4] or MAGP-1. The G_0 and G_∞ values obtained for wild-type

animals in both studies vary from 6.7 x 10^4 Pa to 2.3 x 10^5 Pa, a range broadly comparable to those found in much larger fibers derived from human, bovine, and porcine zonules (1.8 x 10^5 −1.5 x 10^6 Pa)[12, 13, 14, 15, 16]. This agreement among species suggests that these are universal features of these fibers, and gives us confidence that meaningful viscoelastic parameters can be extracted with our method.

A critical step for obtaining quality viscoelastic responses is the orientation of the dissected eye glued to the platform (step 2.1.9). Minor tilting (less than 10°) does not appear to affect the results significantly. Experiments performed outside this limit can generate curves with shapes that deviate from the ones shown in Figure 4. For example, some of those curves may possess two broad peaks instead of one.

Ideally, the procedure outlined in this paper would have been performed without fixation of the eyes, which limits our ability to assess the true viscoelastic parameters of fresh zonular fibers. However, after our preliminary experiments showed no significant difference between the paraformaldehyde-fixed and fresh samples, we decided to adopt fixation as it afforded several advantages. As alluded to in the Protocol, the use of fixed tissues helps to preserve the native stretch of the fibers for the pull-up experiments. Additionally, we found that fixation promoted greater adhesion of the UV glue to the eye capsule, thus reducing the chances of the probe detaching from the lens during the pull-up action, as commonly experienced with fresh samples (probe detachment can be readily recognized as a sudden return of the force to a baseline level). The fixation also prevented buckling of the eyewall in the direction of the pull. Despite this limitation, our method provides a robust approach for determining the relative contribution of protein components to the viscoelastic properties of the zonular fibers.

Although our work to date has focused on the contribution of specific proteins, the method could readily be adapted to study the effect of factors external to the fibers on their mechanical properties. Such factors include temperature, pH, calcium concentration, and the presence or absence of cross-linking enzymes. High-precision measurements could be achieved using our method in differential mode, i.e., by pre-tensioning the zonular fibers with an initial stress/ strain, and then reading the difference in tension that ensues when external conditions are altered. Some of these interventions may conceivably affect the elasticity of the tissues that surround the zonule and hence produce changes in tension that compete with those generated in the zonule. Control measurements with isolated tissues would be needed to assess their relevance to the proposed experiments. We expect that such effects may be negligible, based on observations with the side camera showing that contiguous tissues behave as highly stiff materials that undergo essentially no deformation even when the zonular fibers are fully stretched.

Acknowledgments

This work was supported by NIH R01 EY029130 (S.B.) and P30 EY002687 (S.B.), R01 HL53325 and the Ines Mandl Research Foundation (R.P.M.), the Marfan Foundation, and an unrestricted grant to the Department of Ophthalmology and Visual Sciences at Washington University from Research to Prevent Blindness. J.R. also received a grant from the University of Health Sciences and Pharmacy in support of this project.

References

1. Bassnett S, Shi Y, Vrensen GF Biological glass: structural determinants of eye lens transparency. Philosophical Transactions of the Royal Society B Biological Sciences. 366 (1568), 1250–1264 (2011).
2. Bassnett S Zinn's zonule. Progress in Retinal and Eye Research. 82, 100902 (2021). [PubMed: 32980533]
3. Dureau P Pathophysiology of zonular diseases. Current Opinion in Ophthalmology. 19 (1), 27–30 (2008). [PubMed: 18090894]
4. Shi Y et al. Latent-transforming growth factor beta- binding protein-2 (LTBP-2) is required for longevity but not for development of zonular fibers. Matrix Biology. 95, 15–31 (2021). [PubMed: 33039488]
5. Ushiki T Collagen fibers, reticular fibers and elastic fibers. A comprehensive understanding from a morphological viewpoint. Archives of Histology and Cytology. 65 (2), 109–126 (2002). [PubMed: 12164335]
6. Bassnett S A method for preserving and visualizing the three-dimensional structure of the mouse zonule. Experimental Eye Research. 185, 107685 (2019). [PubMed: 31158380]
7. Todorovic V, Rifkin DB LTBPs, more than just an escort service. Journal of Cellular Biochemistry. 113 (2), 410–418 (2012). [PubMed: 22223425]
8. Mecham RP, Gibson MA The microfibril-associated glycoproteins (MAGPs) and the microfibrillar niche. Matrix Biology. 47, 13–33 (2015). [PubMed: 25963142]
9. Hubmacher D, Reinhardt DP, Plesec T, Schenke- Layland K, Apte SS Human eye development is characterized by coordinated expression of fibrillin isoforms. Investigative Ophthalmology & Visual Science. 55 (12), 7934–7944 (2014). [PubMed: 25406291]
10. Inoue T et al. Latent TGF-β binding protein-2 is essential for the development of ciliary zonule microfibrils. Human Molecular Genetics. 23 (21), 5672–5682 (2014). [PubMed: 24908666]
11. De Maria A, Wilmarth PA, David LL, Bassnett S Proteomic analysis of the bovine and human ciliary zonule. Investigative Ophthalmology & Visual Science. 58 (1), 573–585 (2017). [PubMed: 28125844]
12. Wright DM, Duance VC, Wess TJ, Kielty CM, Purslow PP The supramolecular organization of fibrillin-rich microfibrils determines the mechanical properties of bovine zonular filaments. Journal of Experimental Biology. 202 (21), 3011–3020 (1999). [PubMed: 10518482]
13. Bocskai ZI, Sandor GL, Kiss Z, Bojtar I, Nagy ZZ Evaluation of the mechanical behaviour and estimation of the elastic properties of porcine zonular fibres. Journal of Biomechanics. 47 (13), 3264–3271 (2014). [PubMed: 25242131]
14. Fisher RF, The ciliary body in accommodation. Transactions of the Ophthalmological Societies of the United Kingdom. 105 (Pt 2), 208–219 (1986). [PubMed: 3467496]
15. Michael R et al. Elastic properties of human lens zonules as a function of age in presbyopes, Investigative Ophthalmology & Visual Science. 53 (10), 6109–6114 (2012). [PubMed: 22850416]
16. van Alphen GW, Graebel WP, Elasticity of tissues involved in accommodation. Vision Research. 31 (7-8), 1417–1438 (1991). [PubMed: 1891828]
17. Green EM, Mansfield JC, Bell JS, Winlove CP The structure and micromechanics of elastic tissue. Interface Focus. 4 (2), 20130058 (2014). [PubMed: 24748954]
18. Jones W, Rodriguez J, Bassnett S Targeted deletion of fibrillin-1 in the mouse eye results in ectopia lentis and other ocular phenotypes associated with Marfan syndrome. Disease Models & Mechanisms. 12 (1), dmm037283 (2019). [PubMed: 30642872]
19. Weinbaum JS et al. Deficiency in microfibril-associated glycoprotein-1 leads to complex phenotypes in multiple organ systems. Journal of Biological Chemistry. 283 (37), 25533–25543 (2008). [PubMed: 18625713]
20. Comeglio P, Evans AL, Brice G, Cooling RJ, Child AH Identification of FBN1 gene mutations in patients with ectopia lentis and marfanoid habitus. British Journal of Ophthalmology. 86 (12), 1359–1362 (2002). [PubMed: 12446365]

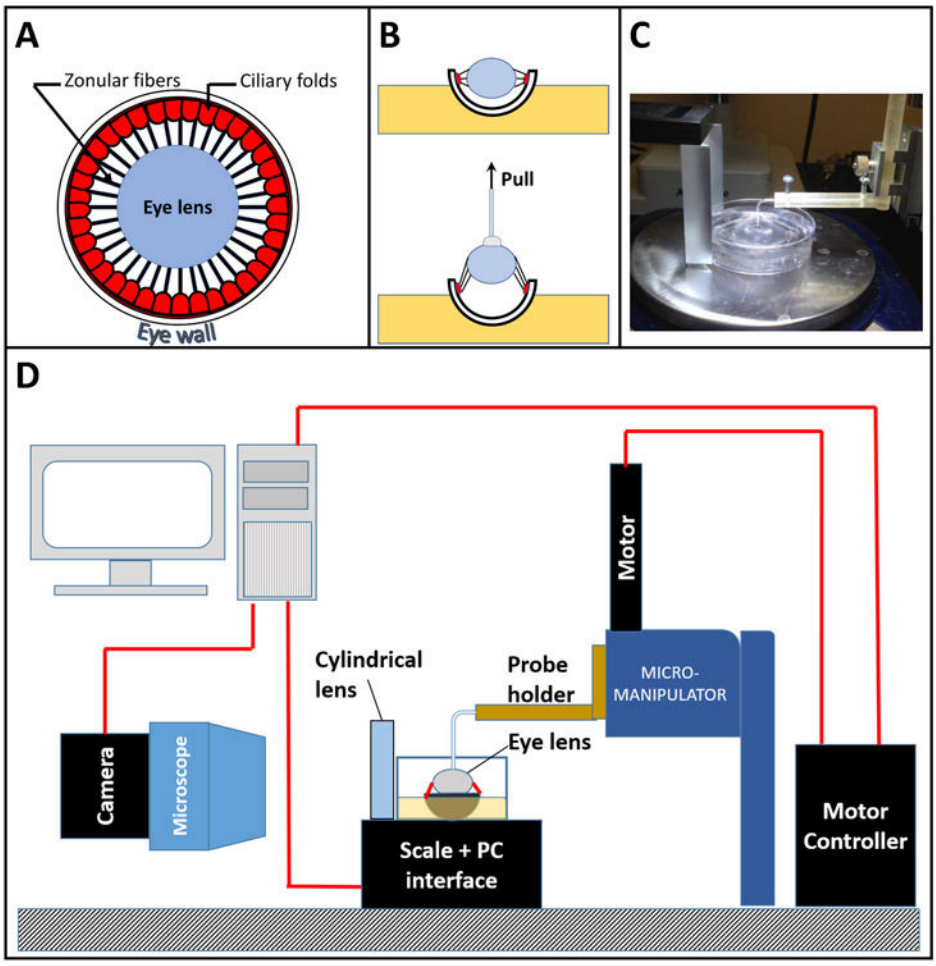

Figure 1: A visual summary of the pull-up method.

(**A**) Cross-sectional view of a vertebrate eye showing the lens and the zonular fibers that suspend it. (**B**) A general approach for determining viscoelastic behavior in zonular fibers by displacing the lens upward (away from the cornea). (**C**) Actual view of a dissected eye glued onto a platform with its lens being pulled upward by a glass probe attached to a micromanipulator. (**D**) Schematic of the entire apparatus.

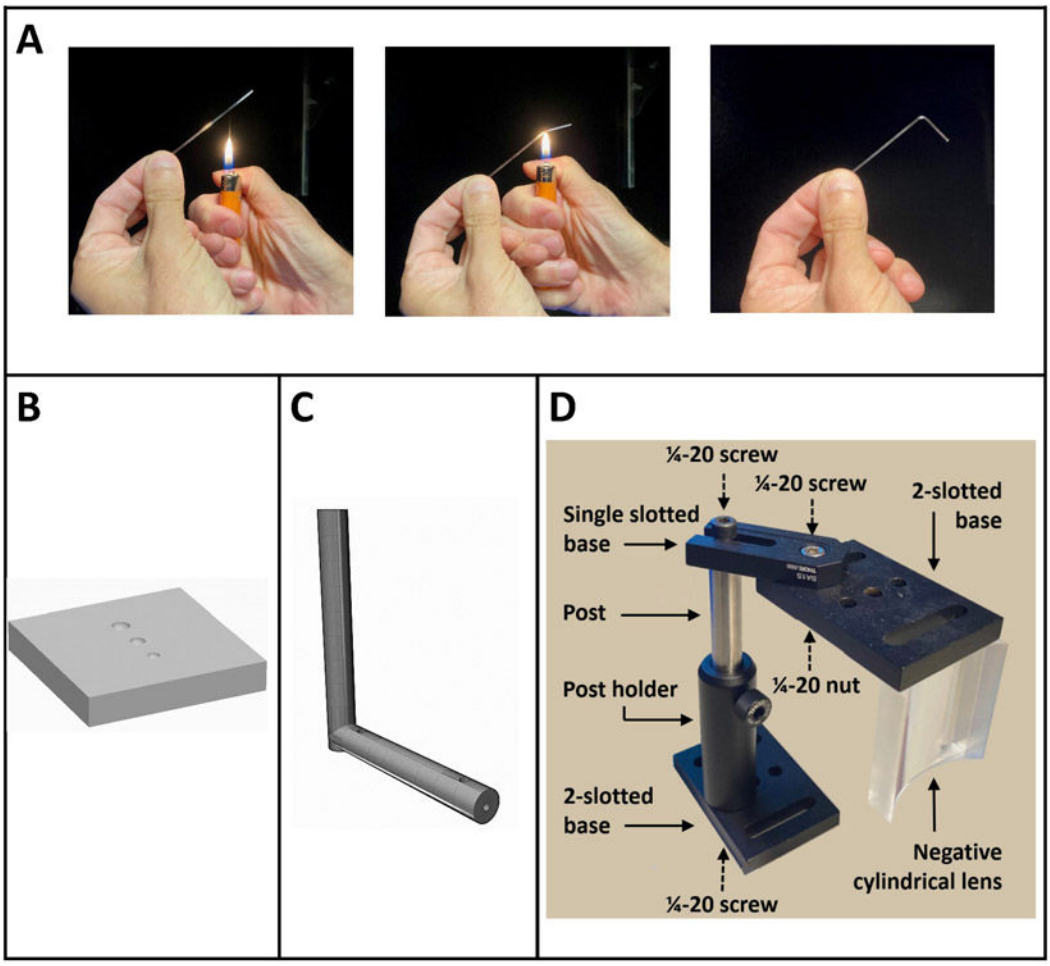

Figure 2: Fabrication of various parts.

(**A**) Fabrication of the glass probe. A glass capillary is held at an angle and a flame is applied at a spot roughly 2 cm from one end. Within a few seconds, the end of the capillary starts to fall. The flame is removed when the end of the capillary is bent at about 90°. (**B**) Fabrication of the eye platform. The part is fabricated with a 3D stereolithography (SLA) printer. It measures 30 x 30 x 5 mm and contains three hemispherical indentations with 2.0, 2.5, and 3.0 mm diameters into which dissected eyes of various sizes are glued. (**C**) Fabrication of probe holder. This part was also fabricated with a 3D SLA printer. It consists of two orthogonal, 7.3 mm diameter rods. The lower rod contains a 1.5 mm bore and two 2.5 mm through holes on the outer surface to accommodate metal screws that secure the capillary probe in place. (**D**) Negative lens assembly. Images captured by the side microscope contain an astigmatic distortion due to the curvature of the Petri dish and the buffer solution. The lens assembly is designed to compensate for the distortion, allowing the side microscope to capture images in sharp focus.

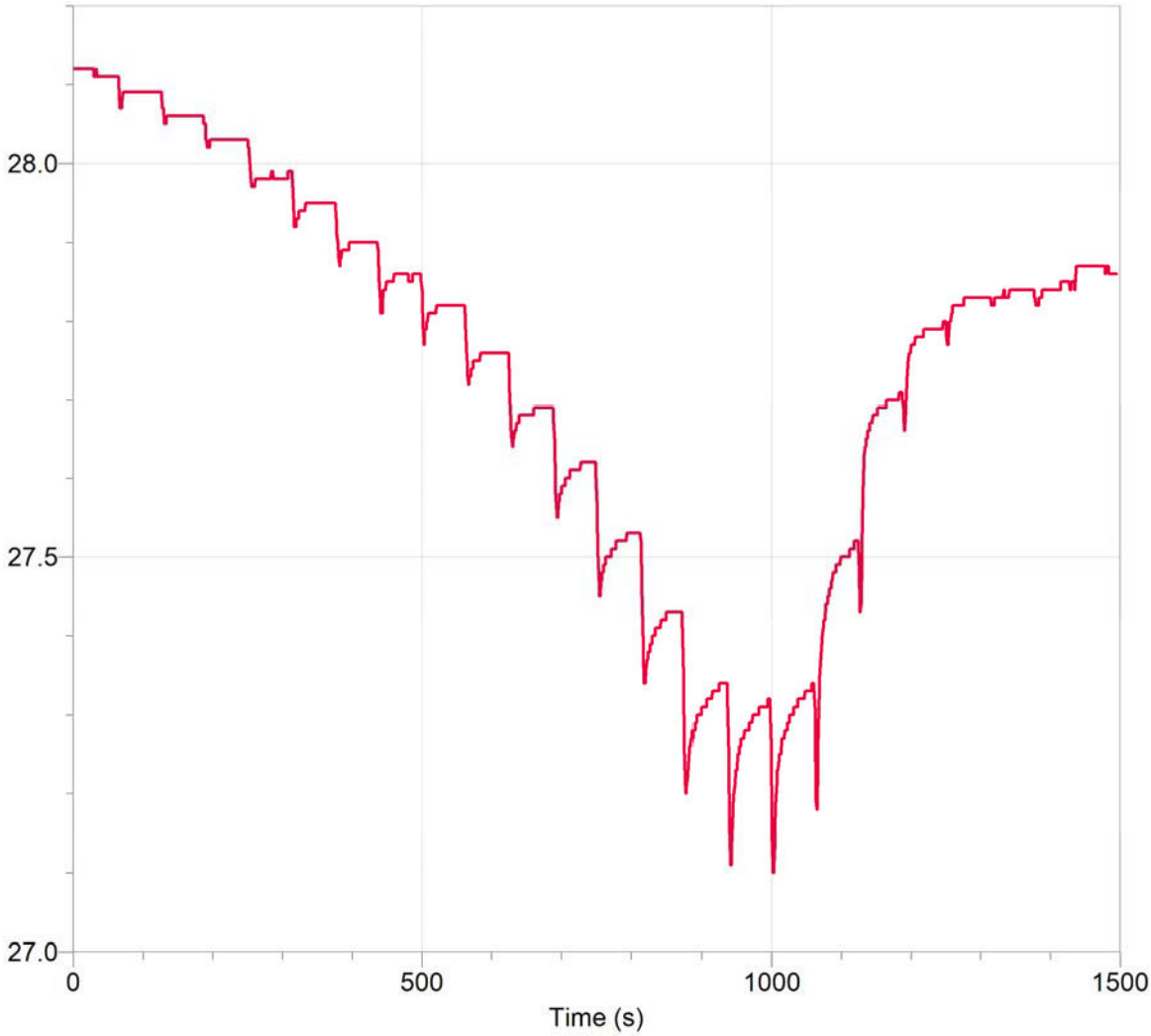

Figure 3: Typical raw data obtained with the assay.

The graph shown was recorded with logging software that records data from a digital scale with a 0.01 g accuracy. The left edge of the graph (time 0) reflects the weight of the sample without a lifting force. The y-axis depicts mass in g. The lens is then lifted in 50 μm steps until all zonular fibers are broken and the Petri dish again rests fully on the scale. Note that the end reading is offset from the initial reading. The offset is due to gradual evaporation of the buffer solution during the course of the experiment and can be accounted for during data analysis, as outlined in step 2.2.14.

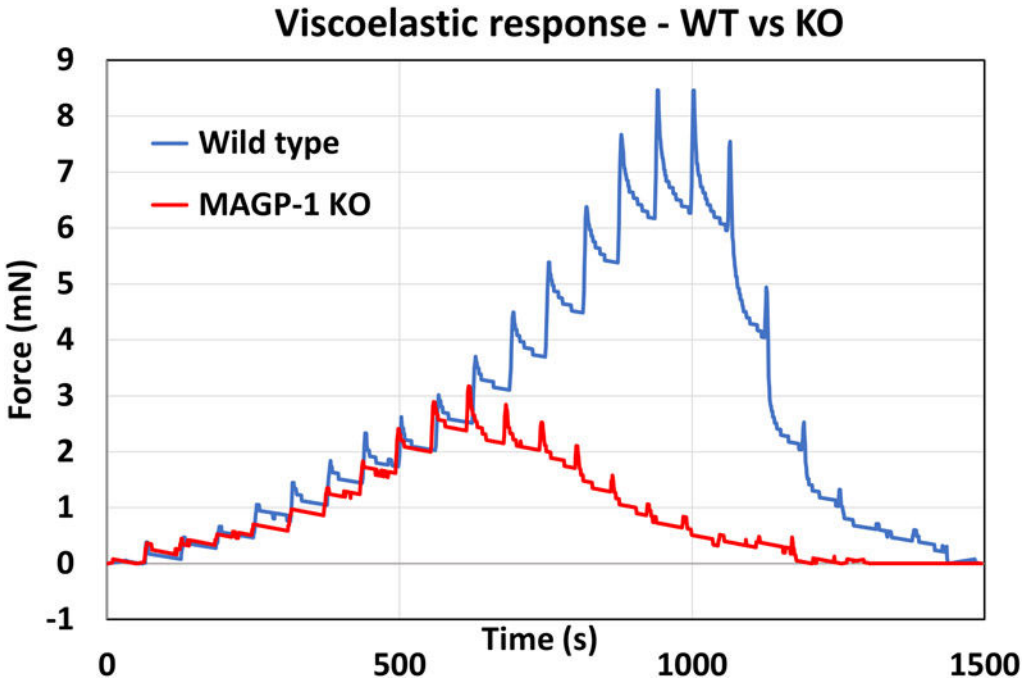

Figure 4: Representative zonular force-displacement curves for wild-type and MAGP-1-deficient mice.

The graph compares the viscoelastic response obtained after discrete displacements of the lens away from its equilibrium position. The response of an eye from a *MAGP-1* knockout (KO) mouse tracks that of an age-matched wild-type animal up to the point where the fibers in the knockout mouse break prematurely.

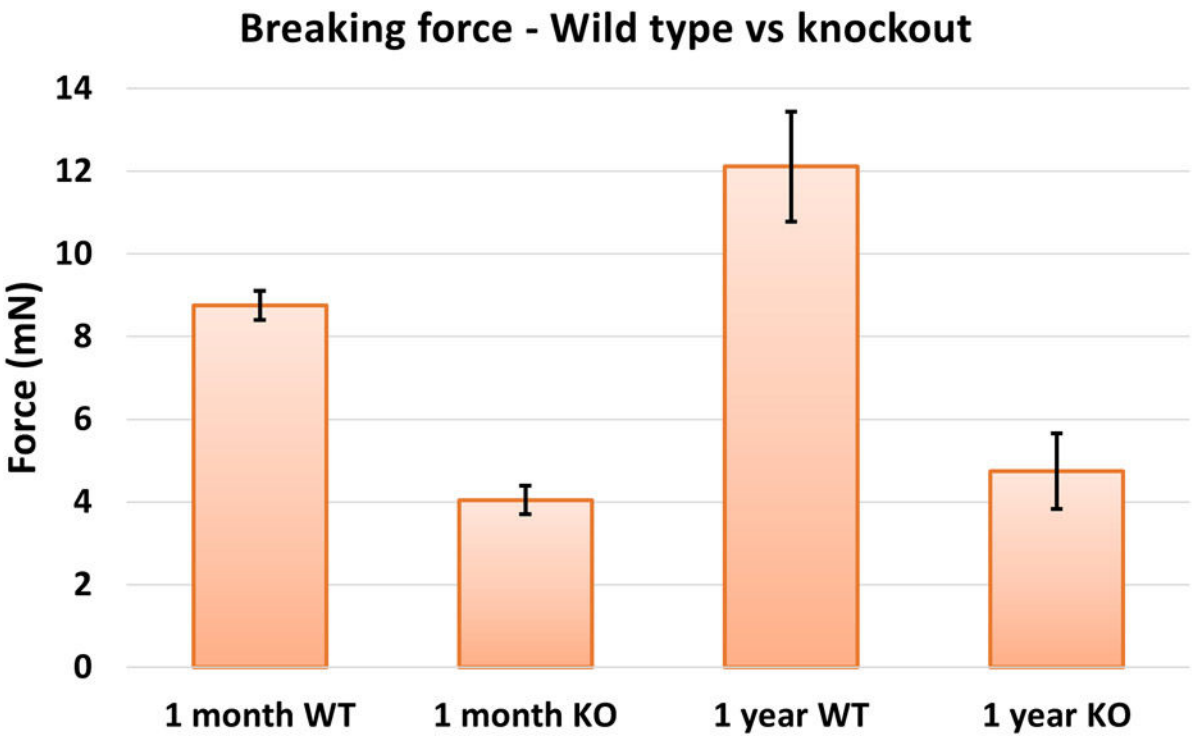

Figure 5: Zonular fiber breaking forces obtained with the pull-up method for *MAGP-1* KO versus wild-type miceand at two ages.

All measurements shown are based on n = 5 or 6 eyes, with error bars representing the standard error of the mean (SEM). Abbreviations: WT = wild-type; KO = *MAGP-1* knockout.

Table 1:
Viscoelastic properties obtained with a quasi-linear viscoelastic (QLV) model.

Data scans like those shown in Figure 4 were analyzed with a QLV model developed specifically for the pull-up assay and the mouse zonule. Best fit parameters for the instantaneous (G_0) and equilibrium (G_∞) stiffnesses, the relaxation time constant (τ), and the ultimate tensile strength (σ_f) are shown. Abbreviations: SD = standard deviation; CI = confidence interval.

Genotype/age		G_0 (Pa)	G_∞ (Pa)	τ (sec)	σ_f (Pa)
WT 1-month	MEAN	2.34E+05	9.33E+04	16.3	9.61E+05
	SD	2.83E+04	2.94E+04	3.4	1.25E+05
	95% CI	5.55E+04	5.76E+04	6.7	2.45E+05
KO 1-month	MEAN	2.73E+05	6.74E+04	17.6	4.44E+05
	SD	6.30E+04	2.06E+04	3.8	7.85E+04
	95% CI	1.23E+05	4.03E+04	7.5	1.54E+05
	p values	0.25	0.12	0.58	0.000022
WT 1-year	MEAN	1.98E+05	7.42E+04	17	1.41E+06
	SD	1.17E+05	2.39E+04	9.1	2.44E+05
	95% CI	2.29E+05	4.69E+04	17.9	4.79E+05
KO 1-Year	MEAN	1.70E+04	2.46E+04	12.9	5.05E+05
	SD	9.06E+03	8.04E+03	7.4	1.48E+05
	95% CI	1.78E+04	1.58E+04	14.4	2.91E+05
	p values	0.0063	0.001	0.41	0.000014
p values, age	WT	0.46	0.23	0.85	0.002
	KO	0.0007	0.0068	0.26	0.44